

**Magnetization curves as probes of Monte Carlo simulation of nonequilibrium states**

J. P. Pereira Nunes, M. Bahiana, and C. S. M. Bastos

*Instituto de Física, Universidade Federal do Rio de Janeiro, Caixa Postal 68528, Rio de Janeiro 21941-972, Brazil*

(Received 23 October 2003; published 24 May 2004)

The influence of parameter choice in the Monte Carlo simulation of zero-field-cooled–field-cooled magnetization curves of granular systems is analyzed. The main simulation techniques are summarized and compared, in terms of the determination of macroscopic quantities usually associated with nanoscopic details of the sample.

DOI: 10.1103/PhysRevE.69.056703

PACS number(s): 02.70.Uu, 82.60.Qr, 75.60.Ej, 75.20.–g

**I. INTRODUCTION**

The search for magnetic media capable of storing large amounts of data in small areas has led to the problem of dealing with particles in the superparamagnetic limit [1]. The strong dependence of the magnetization relaxation time of monodomain particles on their volume and anisotropy constant, combined with the existence of distributions of both quantities in real systems, makes the magnetization process of granular systems an interesting problem in the field of nonequilibrium statistical mechanics. One of the experimental tools used to gain information about the nanoscopic structure of the system is the ZFC-FC (zero-field-cooled–field-cooled) curve, which shows the behavior of the system magnetization in the direction of the applied field as the temperature is varied at some chosen rate. As in hysteresis curves, the form of the obtained curve depends on how quickly the external control parameter is changed. From the theoretical point of view, although it is not difficult to qualitatively understand the influence of the nanoscopic details on the measured curves, a curve that quantitatively describes experimental data has not yet been obtained. The theoretical approach to this problem involves three basic steps: obtaining a correct description of the granular system in terms of particle volumes, shapes, and positions; determining the relevant energy contributions; and, supposing that first two steps have been successfully achieved, describing its relaxation process as the temperature is varied. Monte Carlo simulations have been extensively used in this latter step, leading to a great deal of different results depending on the details of the implementation used. This is by no means a surprise, since the Monte Carlo method is compromised to the correct description of equilibrium states only, and its use for the studies of dynamical problems introduces an artificial time scale to the problem. Many authors claim that it is possible to relate the time scale in Monte Carlo simulations to the real one [2,3], but we believe that this correspondence is not straightforward, even in the case of noninteracting particles, where, in principle, one is able to calculate the energy profile of the sample. If dipolar interaction is included, the correspondence is virtually impossible due to the complicated energy landscape.

In this paper, we summarize and compare some of the main simulation techniques used in this problem, depicting how macroscopic observations are influenced by the chosen scheme. We consider the usual Metropolis and Glauber dy-

namics combined with different choices for the states accessible to Monte Carlo moves, applied to the simulation of ZFC-FC magnetization curves.

Our goal is to determine how the basic features of ZFC-FC curves are affected by different implementations of Monte Carlo simulations of simple noninteracting systems, in order to develop a reliable method for the simulation of systems with dipolar interactions.

**II. SYSTEM AND EXPERIMENT****A. Properties of granular magnetic materials**

A ferromagnetic particle becomes a monodomain when its linear size is below a critical value  $D_c$  determined by the minimization of the total energy, including magnetostatic, exchange, and anisotropy contributions [4]. Below this critical size, the energy associated with the creation of magnetic domain walls is larger than the decrease in the magnetostatic energy due to the smaller total magnetization. Such monodomain ferromagnetic particles can be viewed as large magnetic units, each having a magnetic moment of hundreds of Bohr magnetons.

Systems with superparamagnetic particles may be fabricated by various methods [5–7]. For example, magnetic nanoparticles are spontaneously formed when an alloy containing magnetic atoms, such as  $\text{Cu}_x\text{Co}_{1-x}$  with  $x=0.9$ , is rapidly quenched to a point inside or near the metastable region of the miscibility gap. An example of this process is the fabrication of melt spun ribbons of  $\text{Cu}_{0.9}\text{Co}_{0.1}$ . After a thermal treatment the ribbon is basically composed of magnetic Co particles with a distribution of volumes approximately log-normal, in a nonmagnetic Cu matrix. The average volume, and the width of the volume distribution, as well as the shape of the particles depend in a noncontrolled way on the thermal treatment applied. Usually, in low concentration alloys, neighboring particles are separated by 10–30 nm, and direct exchange, as well as indirect, between particles is neglected [8]. The magnetic properties of such an assembly of nanoparticles are basically determined by the dipolar interaction energy among particles, along with thermal and magnetic anisotropy energies [1]. Although simple to fabricate, granular alloy systems present several complications due to the fact that the volume distribution is itself a metastable state, which may be difficult to reproduce. Simpler samples can be obtained by controlled deposition [5,6,9,10]. In these samples the size, shape, and position of the particles

are more easily determined, and the influence of these aspects may be understood more directly. In this paper we consider mainly the second type of sample. The possibility of a volume distribution, similar to the one in granular alloys, is considered for comparison in some cases. The effect of the dipolar interaction is not yet well understood. There are contradictory experimental results about the dependence of the reversal time for the magnetic moment on the strength of the interaction [9,11–13]. For this reason we consider only samples in which the dipolar interaction may be neglected.

In the simplest case, the particles have uniaxial anisotropy, and each particle is described by its magnetic moment  $\vec{m}_i$ , the direction of the easy magnetization axis,  $\hat{e}_i$ , and its anisotropy constant  $K_i$ . In the presence of an external magnetic field  $\vec{H}$ , the energy for a system of  $N_p$  particles can be written as

$$E = \sum_i^{N_p} \left[ -\vec{m}_i \cdot \vec{H} - \kappa_i \left( \frac{\vec{m}_i \cdot \hat{e}_i}{m_i} \right)^2 \right], \quad (1)$$

where  $\kappa_i = K_i V_i$ , and  $V_i$  is the volume of particle  $i$ . A more significant form for the energy is given in terms of the effective field,

$$E = - \sum_i^{N_p} \vec{m}_i \cdot \vec{H}_i^{\text{eff}}, \quad (2)$$

where

$$\vec{H}_i^{\text{eff}} = \vec{H} + \kappa_i \frac{\vec{m}_i \cdot \hat{e}_i}{m_i^2} \hat{e}_i. \quad (3)$$

Such particles are exposed to a double well potential, corresponding to the two possible orientations along the easy magnetization axis. For zero applied field, reorientation of the magnetic moment, along the easy magnetization axis direction, involves overcoming an energy barrier  $E_b = KV$ . The characteristic time  $\tau$  for switching between energy minima is given by the Arrhenius law  $\tau = \tau_0 \exp(E_b/k_B T)$ , where  $\tau_0 \approx 10^{-9}$  s [14],  $k_B$  is the Boltzmann constant, and  $T$  is the temperature. The relaxation time is strongly dependent on the product  $KV$ , for example, for a spherical Co particle at room temperature,  $\tau$  may vary from 0.1 s for a particle with a 6.8 nm diameter, to 100 yr for a 9.0 nm diameter particle. This means that, for a sample with particles obeying some volume distribution law, for an observation time of 100 s, typical of magnetization measurements, part of the particles will be essentially blocked in one of the minima, while others will be randomly switching between minima, thus showing superparamagnetic behavior. The ZFC-FC magnetization curves are a direct manifestation of this complex behavior.

### B. ZFC-FC magnetization curves

For the ZFC curve the system is initially demagnetized at a sufficiently low temperature, such that  $k_B T \ll E_b$ . Usually experimental curves start at a temperature of a few kelvins. A small magnetic field is applied, and the temperature is increased until the magnetization has dropped to zero, usually

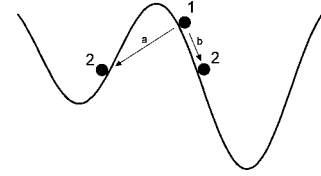


FIG. 1. Energy landscape of a typical magnetic nanoparticle subject to an external field. If the magnetic moment has an initial orientation corresponding to state 1, nonrestricted Monte Carlo moves, such as the ones labeled  $a$  and  $b$ , may be equally probable, and are accepted with probability 1 in the Metropolis implementation.

going up to room temperature, at a typical rate of 1–2 K per minute. Ideally, the FC curve is obtained in the same way, just starting from a state resulting from slowly cooling the system with the applied field. In this sense, the only difference between the curves is the initial state, in the ZFC curve both minima are equally populated in the beginning, while in the FC curve particles are blocked in the global minimum. The experimental realization of the FC initial state may not be possible, as the relaxation times are extremely large at low temperatures. In practice, experimentalists obtain the FC curve starting from a demagnetized state at the end of the ZFC curve, by cooling down the system with the same rate it was previously heated. In both curves the magnetization is recorded at fixed intervals of temperature, or time.

The analysis of ZFC curves usually involves two temperatures,  $T_M$  and  $T_{irr}$ , defined as the temperature at the maximum magnetization in the ZFC curve and the temperature above which the system shows thermodynamic equilibrium properties corresponding to a superparamagnetic behavior, respectively [12]. For a granular system with an applied field two energy barriers are relevant:  $E_{b+}$  between the global minimum and the maximum, and  $E_{b-}$  between the metastable minimum and maximum, as shown in Fig 1. The initial state of the ZFC curve, after the field has been turned on, corresponds to having both minima with equal populations, so a considerable amount of particles are in the metastable state. As the temperature is increased, and the thermal energy becomes first comparable to the smaller values of  $E_{b-}$ , the system magnetization rises as those particles relax and become blocked in their global minimum. This process continues and, as the temperature increases, particles with larger values of  $E_{b-}$  relax, until the magnetization reaches a maximum value at  $T = T_M$ . When the temperature increases past  $T_M$ , particles that have already been equilibrated may have enough energy to overcome  $E_{b+}$  and become magnetically unstable, decreasing the value of the system magnetization. For temperatures larger than  $T_{irr}$ , almost all particles are magnetically unstable, and the system may be considered in thermodynamic equilibrium. For  $T < T_{irr}$  the curves diverge, since the state at  $T = T_{irr}$  is reached from a nonequilibrium situation in the ZFC curve, in which an appreciable number of particles is blocked in the metastable minimum. For  $T > T_{irr}$ , the relaxation time for the magnetization of the particle with the largest value of  $KV$  is much smaller than the typical measuring time, and the ZFC and FC curves coincide. The whole point of this experience is to obtain information

about the nanoscopic structure of the sample, by analyzing the overall shape of the curves and by determining the values of  $T_M$  and  $T_{irr}$ . The width of the ZFC curve may be directly associated with the existence of a volume distribution, which may be derived from the experimental curve. The existence of a plateau at the low-temperature region of the FC curve is usually considered to be of a spin glass phase due to dipolar interaction. The value of  $T_M$  is, in general, defined as an overall blocking temperature of the system. For ZFC and FC curves initiated from equilibrium configurations,  $k_B T_M$  and  $k_B T_{irr}$  are measures of the smaller and larger values of  $E_{b+}$ , respectively.

### III. MONTE CARLO SIMULATIONS OF THE ZFC-FC CURVES

The ZFC-FC curves correspond to sequences of nonequilibrium states of the system, therefore, they are dependent on the temperature variation rate, which means that having the correct Hamiltonian is not enough for a faithful MC simulation. Suppose the typical energy profile for a magnetic moment, as shown in Fig. 1. If a new orientation is sorted without any restriction, flipping between the two energy minima may occur and relaxation is very fast. Also, the transitions  $a$  and  $b$  indicated in Fig. 1 become equivalent, and will be accepted with the same probability since they correspond to the same decrease in energy. Since one is concerned with the correct time scale, this situation is undesirable. Flipping between energy minima may be eliminated through a convenient definition of energy variation [15], but the amplitude of Monte Carlo move, even inside one of the energy wells, is also a concern. It is reasonable to suppose that the new orientation should be chosen from a certain neighborhood, specially in the low-temperature region where blocking is more relevant. Angular restrictions have been implemented in the literature [2,16–21] according to two basic schemes which we will call polar angle restriction (PAR) and solid angle restriction (SAR), from now on. The use of restriction in the Monte Carlo move is well known in the treatment of models with continuous degrees of freedom, such as the  $XY$  and Heisenberg models [22]. For the discussion that follows, we consider that the external magnetic field is in the  $z$  direction, and the orientation of the magnetic moment can be defined by the polar and azimuthal angles  $\theta$  and  $\phi$ , as usual.

The PAR scheme has been used mainly by Porto and collaborators [16–19], the idea being that the magnetic moment, in equilibrium, should precess about the direction of the external field. The new orientation corresponds to a choice of the new angles from uniform distributions defined in the intervals  $[0, 2\pi]$  for  $\phi$ , and  $[\theta - \delta\theta/2, \theta + \delta\theta/2]$  for  $\theta$ . The value of  $\delta\theta$  defines the angular restriction and limits the accessible states that are chosen.

The relaxation towards the direction of the external field is rather artificial, since the easy magnetization axis, in general, will not coincide with the field direction, specially because ZFC-FC curves are obtained with small external fields. The role of the magnetic field in these curves is basically to provide a preferred orientation as close as possible to the easy magnetization axis. One could, instead, adapt the PAR

scheme only considering the direction of the effective field, as defined in Eq. (1) [4]. But, since the effective field also depends on the magnetic moment orientation, this would require the calculation of the effective field direction for each particle, at every attempted move, increasing considerably the computational time.

In the second option of angular restriction, the SAR scheme, the new orientation is chosen within a solid angle centered at the initial direction. The choice of the aperture angle is critical, if it is too small the particle may always be blocked. This problem does not appear in the PAR scheme because, when choosing the direction of the external field for the precession, in fact the new direction is being chosen randomly in relation to the magnetic moment direction, and large direction changes may always happen. In Ref. [20] the authors mention that the aperture is readjusted every time the external field or the temperature is changed, in order to maintain a given acceptance rate that optimizes the simulation. In Ref. [2] the aperture is related to the temperature and an intrinsic time interval, such that it is possible to adjust the aperture at a given temperature in order to obtain a given correspondence between real time and Monte Carlo steps, and vice versa. Still, the optimization of the Monte Carlo simulation is used as a criterion for the choice of aperture angle. Since our goal is to examine how the choice of simulation parameters influences the resulting curves, we simply choose a certain value of solid angle, which is kept constant along the magnetization curve.

### IV. RESULTS

In order to compare the different schemes listed above, we have considered a system of 400 noninteracting particles with magnetic moment  $869\mu_B$ , anisotropy constant  $1.32 \times 10^6$  erg/cm<sup>3</sup>, anisotropy axis sorted from a uniform distribution, subject to an external field of 0.1 kOe in the  $z$  direction. Such values are compatible with a sample of  $\text{Cu}_{0.9}\text{Co}_{0.1}$  fabricated by melt spinning [23]. The initial state has the particles' magnetic moment randomly oriented with respect to the anisotropy axis, such that the system magnetization is zero. For the ZFC curve, the initial temperature is 1 K. The particles are sequentially chosen, their magnetic moment rotated with or without restriction, and the new state accepted with a probability depending on the Monte Carlo implementation used.

After  $S$  Monte Carlo steps, or complete updates of the system, the temperature is increased by  $\Delta T = 1$  K, up to 200 K. The temperature is then decreased down to 1 K at the same rate, and the FC curve is collected. The same procedure is repeated 200 times, starting from different choices for the magnetic moments and easy axis orientation. The resulting curves are then averaged. At this point the choice of  $S$  is completely arbitrary, the values used are such that the simulated curves resemble the experimental ones [23]. The value of  $T_{irr}$  may be obtained from the subtraction of the two curves since for  $T < T_{irr}$  the FC magnetization is systematically higher.

We have also performed some simulations with the particle moments distributed according to log-normal distribu-

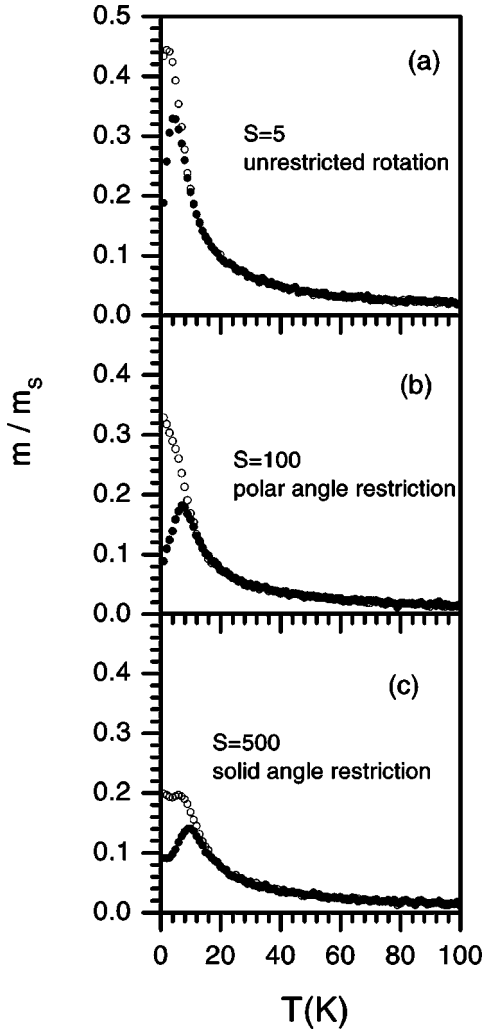


FIG. 2. Magnetization curves simulated according to the Metropolis scheme for three cases: (a) unrestricted rotations and  $S=5$ ; (b) rotations restricted to a band of aperture  $\delta\theta=0.1$  centered on the external field direction (PAR scheme) and  $S=100$ ; (c) rotations restricted to a solid angle centered at the magnetic moment initial direction defined by the angular aperture  $\delta\theta=\delta\phi=0.1$  (SAR scheme) and  $S=500$ .

tion, as is observed in granular alloys, in order to see the effects of this distribution on the ZFC-FC curves.

### A. Metropolis algorithm

After the magnetic moment of the chosen particle is altered, the change in energy ( $\Delta E$ ) due to the new orientation is calculated and the rotation accepted with probability  $p = \min[1, \exp(-\Delta E/k_B T)]$ . Figure 2 shows the resulting curves for nonrestricted rotations and  $S=5$  (a), for the PAR scheme with  $\delta\theta=0.1$  and  $S=100$  (b), and for the SAR scheme with  $S=500$  and  $\delta\phi=\delta\theta=0.1$  (c). In the first case, the nonrestricted rotation leads to a rapid relaxation, such that for  $S > 5$  the FC and ZFC curves coincide. If we use the same number of steps with the restricted schemes, the ZFC magnetization would be too small because the system would be almost completely blocked. We need to use a value for  $S$  at

TABLE I. Variation of  $T_M$  and  $T_{irr}$  with the restriction scheme for the Metropolis dynamics. The external field is 0.1 kOe.

$S$	$T_M$ (K)	$T_{irr}$ (K)
Free	4	8
PAR	7	11
SAR	9	16

least one order of magnitude larger to obtain a comparable curve. Comparing now the PAR and SAR schemes, we notice that in the first one the ZFC curve is higher and narrower. The reason is that the rotation towards the direction of the external field, even when restricted, may lead to large rotations regarding the effective field direction, so the relaxation is faster and the distribution of anisotropy axis is less important. When the rotation is restricted to the solid angle, the alignment of the magnetic moment is slow and particles that start with  $\vec{m}$  pointing in the wrong direction may not relax. Also, the FC curve simulated in the SAR scheme presents a plateau at low temperatures [Fig. 2(b)], usually associated with a spin glass phase in interacting systems. Table I shows the values of  $T_M$  and  $T_{irr}$  for the graphs in Fig. 2.

It is interesting to explore the dependency of the ZFC-FC curves' properties on the choice of  $S$  and amplitude of the angular restriction. We choose the SAR scheme for this study. Figure 3 shows the resulting curves for 100, 500, and 2000 Monte Carlo steps. The corresponding values of  $T_M$  and  $T_{irr}$  are shown in Table II. As  $S$  increases, the values of  $T_M$  and  $T_{irr}$  become closer and the irreversible part of the ZFC curve decreases. It is clear that  $S=2000$  is not adequate for a temperature step of 1 K, since there is no irreversible region, and nothing can be concluded from the simulation. The other curves show plausible results, which differ mainly in the total value of magnetization, and the position of the maximum of the ZFC curve. The discrepancy between the number of Monte Carlo steps used is such that a unique definition of time scale is not possible.

Figure 4 shows the relaxation curves, averaged over 200 realizations, for different values of angular aperture for the SAR scheme. The initial state is chosen with all the magnetic moments aligned in the direction of the external field and the relaxation occurs in the presence of a 0.1 kOe field at a constant temperature of 8 K. The analysis of the figure shows a very strong dependence of the relaxation dynamics on the angular aperture.

### B. Size distribution effects

The effects of a size distribution over the particles remain to be computationally investigated. Real samples typically show a log-normal volume distribution of the form

$$f(V) = \frac{1}{\sqrt{2\pi}\sigma V} \exp\left(-\frac{\ln^2(V/V_0)}{2\sigma^2}\right), \quad (4)$$

where  $\sigma$  is the standard deviation and  $V_0$  is the most probable volume. In agreement with theoretical models [12], we expect to see a wider ZFC peak when the system is not

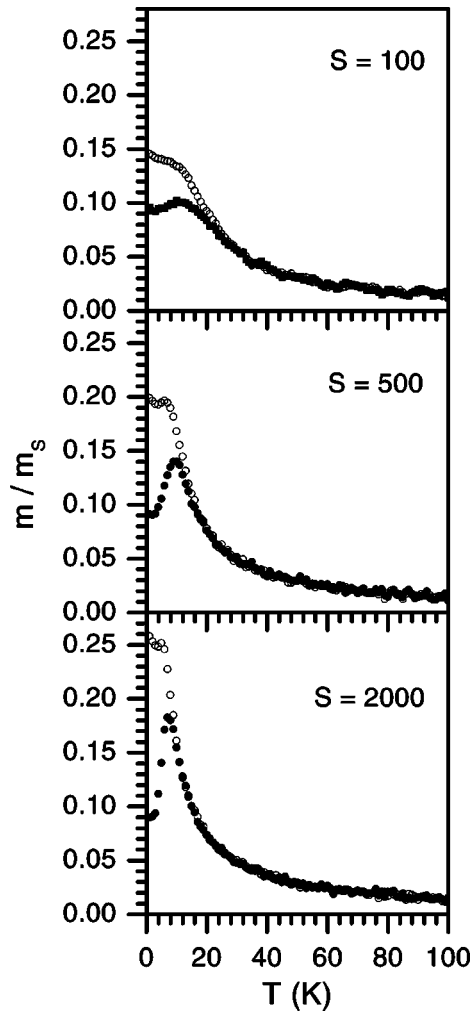


FIG. 3. Influence of the number of Monte Carlo steps on the overall properties of ZFC-FC curves. The curves show the results obtained with the SAR scheme with (a)  $S=100$ , (b)  $S=500$ , and (c)  $S=2000$ .

monodisperse. However, the curves simulated with unrestricted moves are insensitive to the introduction of a volume distribution, as shown in Fig. 5. On the other hand, if the SAR scheme is chosen, a monodisperse system shows no appreciable difference as compared to a system with some volume distribution, as seen in Fig. 6. With the value  $\sigma=0.5$  the presence of particles with  $V=2V_0$  occurs with high probability, and the value of  $T_M$  should reflect the increase in relaxation time, but this is not observed, as seen in Table III.

TABLE II. Variation of  $T_M$  and  $T_{irr}$  with the number of Monte Carlo steps,  $S$ , in the SAR scheme. As  $S$  increases the difference between the two temperatures decreases, indicating that the system becomes superparamagnetic.

$S$	$T_M$ (K)	$T_{irr}$ (K)
100	10	24
500	9	14
2000	7	10

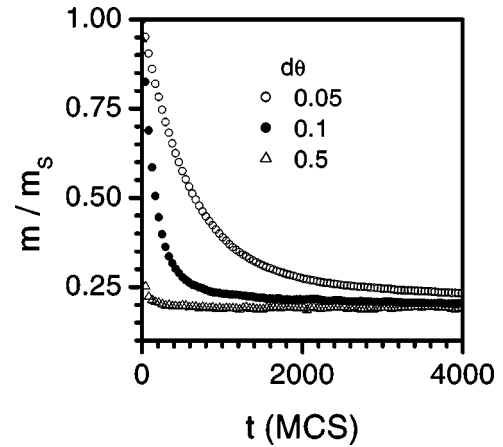


FIG. 4. Relaxation curves for the SAR scheme and temperature equal to 8 K with different values of angular aperture. The relaxation times obtained are clearly different.

### C. Comparison between Metropolis and Glauber dynamics

Finally we compare the Metropolis dynamics with the Glauber dynamics in order to see how this change in the probability of acceptance can influence the qualitative aspect of a ZFC-FC curve (see Figs. 7 and 8).

The Glauber dynamics has been introduced by Glauber in the context of one-dimensional Ising model, its main difference to the Metropolis dynamics is that flips reducing the energy of the particle are not always accepted. In this dynamics the probability of acceptance is commonly written as  $p = [1 - \tanh(-\Delta E/2k_B T)]/2$ . As expected, relaxation curves obtained from each dynamics are different, although the relaxation times obtained are very similar. For this reason there is no clear difference in the ZFC-FC curves obtained with the two dynamics.

## V. DISCUSSION

The results obtained in the preceding section are just a small sample of the variety of choices for this kind of simu-

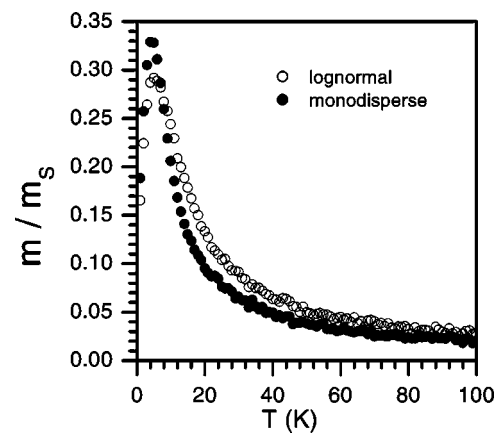


FIG. 5. ZFC-FC curves obtained with Metropolis dynamics with unrestricted rotations for a system with a log-normal distribution for the magnetic moments. The median moment is  $869\mu_B$  and the standard deviation is 1.5. All the others as parameters are common to the monodisperse system.

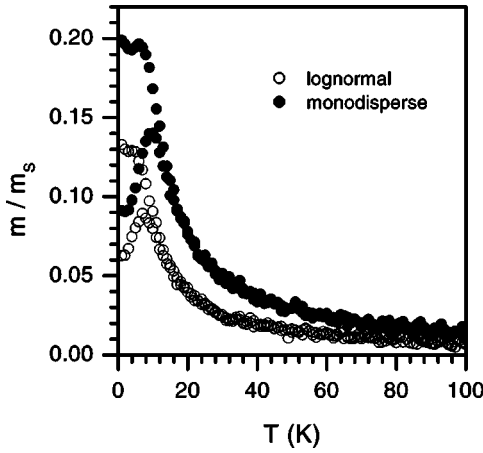


FIG. 6. ZFC-FC curves obtained with Metropolis dynamics with the SAR scheme for a system with a log-normal distribution for the magnetic moments. The median moment is  $869\mu_B$  and the standard deviation is 0.5.  $S=500$  and  $d\theta=d\phi=0.1$  for both systems.

lation. The choice of simulation method and the values of parameters always involve some arbitrariness, and it is clear that the comparison between simulations obtained from different procedures is meaningless. Of course this is not desirable when one has the goal of comparing simulations with real experiments. However, qualitative analysis is possible if some care is taken. For example, the chosen method should be able to achieve equilibrium configurations for some number of steps, and must be sensitive to alterations of the system on the nanoscopic scale. In this sense the unrestricted dynamics fails the second criterion. On the other hand, the choice of angular amplitude in restricted dynamics must be large enough to allow equilibration. The determination of  $d\theta$  may be found by trial and error for the chosen values of volume and anisotropy.

The choice of  $S$  and  $\Delta T$  is important because their values define the heating/cooling rate  $R=\Delta T/S$ . If  $R$  is too small, the system will be able to equilibrate at each value of temperature and the ZFC-FC curves will coincide, but this condition gives only an upper bound for  $R$ . The natural impulse is to use the relaxation curves as calibrations for the time scale, by comparing them with experimental curves. This method was used in Ref. [15] for noninteracting systems, and the result was that the typical time interval of 100 s corresponds to  $10^{14}$  Monte Carlo steps. With this correspondence it would be impossible to simulate ZFC-FC curves, which is inconsistent with the fact that several simulations are reported in the literature. Another possibility for noninteracting systems is to compare the relaxation process via Langevin dynamics and Monte Carlo simulation. This was done in Ref.

TABLE III. Influence of the size distribution over  $T_B$  and  $T_{irr}$ , in the SAR scheme with  $S=500$ .

Distribution	$T_M$ (K)	$T_{irr}$ (K)
Monodisperse	9	16
Log-normal $\sigma=0.5$	7	13

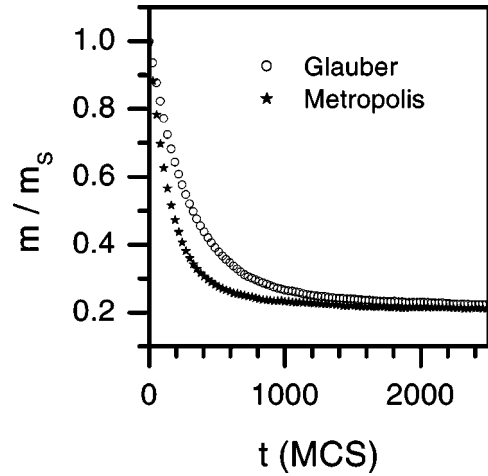


FIG. 7. Comparative plot between the relaxation dynamics using Metropolis and Glauber dynamics in the SAR scheme. The relaxation is made in the presence of a 0.1 kOe external field and the temperature is constant equal to 8 K.

[2] for Monte Carlo simulations with a solid angle restriction. The result was that the cone aperture must be varied with the temperature in order to keep a constant equivalence between real time and one Monte Carlo step, but the absolute value of the proportionality constant cannot be uniquely determined.

The apparent volume distribution found with the SAR scheme can be understood if one examines the initial condition. Since the easy magnetization axes are uniformly distributed, when the external field is applied on the demagnetized system at the beginning of the ZFC curve, the particles' magnetic moments will be randomly oriented with respect to the effective field at each particle, therefore, the energy barrier presented to each particle will vary. For a restricted dynamics the number of steps necessary to overcome the energy barrier will vary from particle to particle, and the resulting ZFC curve will be a reflection of those different relaxation times. If one believes that the restricted Monte Carlo dynamics re-

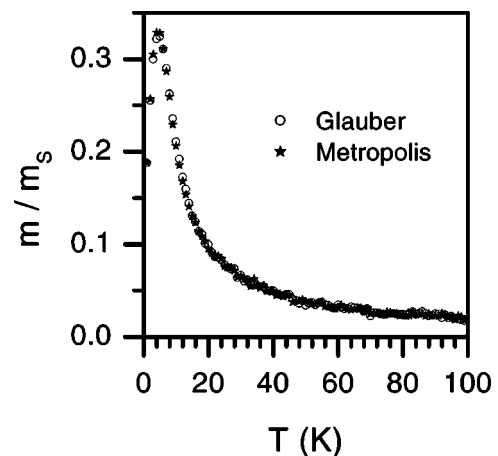


FIG. 8. Comparative plot between ZFC-FC curves obtained using Metropolis and Glauber dynamics in the unrestricted rotation scheme. There is no apparent difference between the results of the two dynamics.

sembles the actual dynamics in real systems, then the same distribution of relaxation times occurs even in monodisperse systems, and the derivation of the volume distribution from the ZFC curve may not reflect the actual volume distribution in the sample. Also, the development of a plateau at low temperatures in FC curves, usually an indication of the relevance of dipolar interactions in the sample, may be a consequence of the restricted dynamics. A good test would be obtaining a ZFC curve for a monodisperse system, or for a system with a well known volume distribution, and calculating the apparent volume distribution from the ZFC.

In conclusion, we believe that the Monte Carlo simulation still is a valuable tool for qualitative analysis of nonequilibrium magnetization curves. The direct comparison of absolute values of blocking temperatures from experiments and simulations is not possible since the choice of simulation parameters strongly affects the shape of the curves. It is cru-

cial to start with a system that minimally resembles the real one, regarding values of volume, anisotropy, and spacing if dipolar interactions are considered. Working with adimensional Hamiltonians may lead to systems with distinct dynamical regimes as compared to typical granular samples. Unrestricted dynamics are definitely not adequate to the simulation of nonequilibrium magnetization curves. Having in mind that the ultimate goal is the simulation of interacting systems, we find that the SAR scheme provides a reasonably realistic dynamics, if care is taken in the choice of the angular aperture.

#### ACKNOWLEDGMENTS

The authors acknowledge the support from FAPERJ, CNPq, CAPES, and Instituto de Nanociências/MCT.

- 
- [1] X. Batlle and A. Labarta, *J. Phys. D* **35**, R15 (2002).
  - [2] U. Nowak, R.W. Chantrell, and E.C. Kennedy, *Phys. Rev. Lett.* **84**, 163 (2000).
  - [3] P. Vargas, M. Knobel, and D. Altbir, *Z. Metallkd.* **93**, 974 (2002).
  - [4] G. Bertotti, *Hysteresis in Magnetism; For Physicists, Materials Scientists, and Engineers* (Academic Press, New York, 1998).
  - [5] H.T. Yang, C.M. Shen, Y.K. Su, T.Z. Yang, H.J. Gao, and Y.G. Wang, *Appl. Phys. Lett.* **82**, 4729 (2003).
  - [6] J.I. Martn, J. Nogus, K. Liu, J.L. Vicent, and I. K. Schuller, *J. Magn. Magn. Mater.* **256**, 449 (2003).
  - [7] E.C.S. da Silva, M. Knobel, E.F. Ferrari, J.C. Denardin Jand, M.G.M. Miranda, G.J. Bracho, A.B. Antunes, and M.N. Baibich, *IEEE Trans. Magn.* **36**, 3041 (2000).
  - [8] D. Altbir, P. Vargas, and J. d' Albuquerque e Castro, *Phys. Rev. B* **54**, R6823 (1996).
  - [9] F. Luis, F. Petroff, J.M. Torres, L.M. Garcia, J. Bartolomé, J. Carrey, and A. Vaurés, *Phys. Rev. Lett.* **88**, 217205 (2002).
  - [10] R.P. Cowburn, A.O. Adeyeye, and M.E. Welland, *New J. Phys.* **1**, 1 (1999).
  - [11] M. El-Hilo, K. O'Grady, and R.W. Chantrell, *J. Appl. Phys.* **76**, 6811 (1994).
  - [12] J.L. Dormann, D. Fiorani, and E. Tronc, *Adv. Chem. Phys.* **XCVIII**, 283 (1997).
  - [13] S. Mørup and E. Tronc, *Phys. Rev. Lett.* **72**, 3278 (1994).
  - [14] B.D. Cullity, *Introduction to Magnetic Materials* (Addison-Wesley, Reading, MA, 1972).
  - [15] P. Vargas and D. Altbir, *J. Magn. Magn. Mater.* **167**, 161 (1997).
  - [16] J. García-Otero, M. Porto, J. Rivas, and A. Bunde, *J. Appl. Phys.* **85**, 2287 (1999).
  - [17] J. García-Otero, M. Porto, J. Rivas, and A. Bunde, *Phys. Rev. Lett.* **84**, 167 (2000).
  - [18] J. García-Otero, M. Porto, J. Rivas, and A. Bunde, *J. Appl. Phys.* **87**, 7376 (2000).
  - [19] M. Porto, *Eur. Phys. J. B* **26**, 229 (2002).
  - [20] D.A. Dimitrov and G.M. Wysin, *Phys. Rev. B* **54**, 9237 (1996).
  - [21] D. Hinzke and U. Nowak, *Comput. Phys. Commun.* **121**, 334 (1999).
  - [22] M.E.J. Newman and G.T. Barkena, *Monte Carlo Methods in Statistical Physics* (Oxford University Press, Oxford, NY, 2001).
  - [23] C.S.M. Bastos, W.C. Nunes, M. Bahiana, M.A. Novak, D. Altbir, P. Vargas, and M. Knobel, *Phys. Rev. B* **66**, 214407 (2002).